UC Santa Cruz
UC Santa Cruz Previously Published Works

Title
Unusual Structure and Dynamics at Silica/Methanol and Silica/Ethanol Interfaces□A Molecular Dynamics and Nonlinear Optical Study

Permalink
https://escholarship.org/uc/item/4bn7v57f

Journal
The Journal of Physical Chemistry B, 120(8)

ISSN
1520-6106

Authors
Karnes, John J
Gobrogge, Eric A
Walker, Robert A
et al.

Publication Date
2016-03-03

DOI
10.1021/acs.jpcb.5b07777

Peer reviewed

Unusual Structure and Dynamics at Silica/Methanol and Silica/Ethanol Interfaces – A Molecular Dynamics and Nonlinear Optical Study

John J. Karnes[1], Eric A. Gobrogge[2], Robert A. Walker[2,*], and Ilan Benjamin[1,*]

[1]Department of Chemistry and Biochemistry, University of California-Santa Cruz, Santa Cruz, CA, 95064.

[2]Department of Chemistry and Biochemistry, Montana State University, Bozeman, MT 59715.

KEYWORDS: solid-liquid interface, hydrogen bonding, solvent polarity, molecular orientation

*corresponding authors:

rawalker@chemistry.montana.edu, 406-994-7928

benjamin@chemistry.ucsc.edu, 831-459-3152

ABSTRACT

Vibrational sum frequency (VSF) spectroscopy and molecular dynamics simulations are used to investigate ethanol-silica and methanol-silica interfaces. We describe the subtle differences in molecular organization that result in different VSF spectra obtained at the alcohol-silica liquid-solid interfaces. Alcohol molecules hydrogen bonded to the silica surface induce orientational opposition in an adjacent low-population region, which implies VSF signal reduction. This low population region is essentially of zero density in the ethanol system, suggesting less signal cancellation. Simulated silica defect sites increase the population of this region in both systems. Interestingly, the induced orientation in this region influences subsequent molecular orientation only in the ethanol-silica system, preserving the interfacial anisotropy. These effects suggest a stronger VSF response from the ethanol-silica system versus the methanol-silica system, where more methanol molecules reside in the low-population region and this region does not induce order in subsequent solvent layers.

I. INTRODUCTION

Solid surfaces often force molecules in an adjacent phase to adopt anisotropic structures and organizations leading to differences between bulk and interfacial properties. Both experimental and computational studies of these surfaces have shown distinctive changes in interfacial density, dynamics, and solvation relative to bulk behavior.[1-6] These changes have direct consequences for mechanistic descriptions of a wide array of surface phenomena including adhesion, corrosion, chromatography, and catalysis.[7-11] Traditionally these properties have been

studied using linear spectroscopic[12] and wet chemical methods,[13] but more recently, nonlinear optical methods have aided in characterizing chemical structure, organization and reactivity in these asymmetric environments.[1, 14, 15]

Acetonitrile is one example of a solvent with well-studied interfacial behavior. Weeks and co-workers studied the silica/acetonitrile interface using both vibrational sum frequency spectroscopy (VSFS) and molecular dynamics (MD) simulations.[16] The results of both the experimental and theoretical studies indicated an interfacial structure varying greatly from that of the bulk. Simulations predicted that acetonitrile formed a bilayer structure at the interface, and that this bilayer structure of oppositely oriented acetonitrile molecules extended several nanometers into the bulk. VSFS experiments support this picture and imply that the first sublayer interacting directly with the silica surface has vibrational structure that is slightly different from acetonitrile oriented in the opposite direction and not closely associated with the silica. The silica/water interface has also been well studied.[15, 17-19] These studies show that interfacial water molecules can exist in two different environments. One environment involves tetrahedrally coordinated water molecules while the other involves water in a more weakly associated hydrogen-bonding environment. Furthermore, these studies showed that the molecules' environment was highly dependent on solution pH. Unique interfacial organization has also been found at the silica/1-alcohol interface. Shen and co-workers determined that for C1-C4 alcohols, the molecules at the silica/vapor interface adsorbed with their methyl groups oriented away from the surface. The decrease in signal observed at the silica/liquid interface was explained by the formation of a bilayer between oppositely oriented molecules.[20]

Alcohol adsorption to solid substrates is of particular interest due to industry's use of oxide catalysts in the production of alkenes, esters, ethers, aldehydes, alkylamines,[21] and

blending compounds for reformulated gasoline.[22, 23] Numerous experimental and theoretical studies have investigated both these solid/alcohol and solid/alcohol vapor interfaces.[23-26] More recently, VSFS and other 2nd order nonlinear optical methods have been employed to study molecular-level interactions at buried silica/liquid alcohol interfaces.[20, 27-32] Using this surface specific technique, vibrational modes of species in asymmetric environments have been observed and used to discern the structure and organization of interfacial molecules. Of all the short chain alcohols, methanol exhibits the most peculiar behavior, with data from experiments and simulations leading to conflicting descriptions of solvent structure at this solid/liquid interface.

While VSFS studies have reported strong methanol signatures from silica/methanol vapor interfaces, signal at the silica/methanol interface is virtually nonexistent.[20, 27, 28] Shen and co-workers accredited this observation to the proposed formation of a rigid methanol bilayer at the interface with the first sublayer hydrogen bonding to the surface silanols, and the second sublayer interacting weakly through the opposing methyl groups. Due to the opposing methyl groups having antiparallel vibrational dipoles, the SF signal was predicted to disappear.[20] This same cancellation, however, is not seen when the methanol is replaced with ethanol. Ethanol has an observable VSFS response at both the silica/vapor and silica/liquid interfaces.[20] While the silica/vapor signal arises from the same hydrogen-bound monolayer, the bilayer observed at the silica/liquid interface does not result in complete cancelation of SF signature. This observation is accredited to two main sources. First, the second layer is expected to have a much broader orientational distribution than the first layer; and second, while the methyl symmetric stretches of the two layers are oppositely oriented and result in severely diminished signal, the antisymmetric stretches remain unaffected.[20] Further attempts at characterizing these surfaces have been made

by examining binary mixtures of the alcohol with water, carbon tetrachloride, and acetonitrile.[27, 28]

Methanol *will* give rise to a signal at silica/liquid interfaces under carefully controlled conditions. Zhang *et al.* have studied both methanol-water and methanol-carbon tetrachloride binary mixtures at the silica interface using VSFS. They found that in binary solutions with CCl_4, methanol gave a strong SF signal at methanol mole fractions of 3-30%, but at higher fractions, the signal disappeared. When carbon tetrachloride was replaced with water, however, methanol did not give a signal at any mole fraction.[28] These behaviors were attributed to the nonpolar nature of carbon tetrachloride allowing the formation of a methanol monolayer at the surface until a high enough mole fraction is reached and a second antiparallel methanol sublayer forms. In water, however, methanol molecules are forced through hydrophobic interactions to associate through the methyl groups at all mole fractions resulting in no SF signal. In a similar experiment, Gobrogge and Walker studied binary mixtures of methanol and acetonitrile and found that any response from methanol was conspicuously absent at all mole fractions, further supporting the proposed model of interfacial methanol pairs consisting of oppositely oriented monomers.[27]

Computational studies have also been used to investigate the silica/alcohol buried interface. Roy *et al.* confirmed that at the silica/methanol interface, the first sublayer of methanol molecules hydrogen bonds strongly to the surface silanol groups, but found that the second sublayer tends to associate with the O-H bonds pointing towards the surface.[5] Simulations suggest that the second sublayer forms additional hydrogen bonds with the first sublayer as opposed to interacting through the van der Waals attraction of antiparallel methyl groups. Such organization should lead to *enhanced* SF intensity given that interfacial solvent molecules are all oriented in approximately the same direction. However, computational support is also found for

the antiparallel bilayer model. Simulations by Tallarek and co-workers show that methanol forms a monolayer hydrogen bound to the silanols thereby presenting a hydrophobic surface to the bulk. The methyl-terminated interface then causes the next layer of methanol molecules to orient their methyl groups toward the surface.[33] Such organization should lead to significantly diminished (or absent) signals in VSFS experiments consistent with what has been observed experimentally.

Differences between these two descriptions of methanol organization are likely to be sensitive to experimental conditions including surface silanol density. Specifically, if the surface silanol density is high and the surface layer of methanol is packed tightly, one might expect that the second layer of methanol to adopt an antiparallel arrangement. However, if the silanol surface coverage is lower, adsorbed methanol monomers will have enough space in between so that the second layer can hydrogen bond to the first.

In the work presented below, results from molecular dynamics (MD) simulations are compared with data from VSFS experiments in order to develop a better understanding of the structure of methanol and ethanol at the silica interface. Experiments show that while both alcohols give a signal at the silica/vapor interface, only ethanol gives an appreciable signal at the silica/liquid interface. Our MD simulations support the layered methanol system proposed by Roy et al.[5] Striking differences between the two solvents are observed in their organization and dynamics, however. When compared to methanol, ethanol molecules are shown to have longer-lived alcohol-silica hydrogen bonds, and a large (~3 Å) region of near zero density between the first two sublayers. Furthermore, by lowering the number of active sites on the surface and thereby decreasing the number of hydrogen bonded methanol molecules, the density of the second methanol sublayer is shown to *increase* as the surface (including the first methanol layer)

becomes less hydrophobic. While this predicted result is difficult to test systematically by experiment, surface hydroxyl coverage *can* be changed by changing the substrate. α-Alumina has surface hydroxyl concentrations 2-3 times higher than silica. VSF data from the methanol/α-alumina liquid-solid interface show a weak but pronounced response from the interfacial solvent. This result suggests that small changes in surface composition have very strong effects on local solvent organization.

This paper is organized as follows. In parts 2 and 3 we detail the relevant experimental and simulation techniques used to study the silica-methanol and silica-ethanol systems. In part 4 we introduce the system through the viewpoint of MD simulations, describe experimentally obtained VSF spectra, and qualitatively explain interesting features of these spectra by directly comparing MD data from these two systems.

II. EXPERIMENTAL METHODS

Spectroscopic grade methanol and ethanol were obtained from Sigma-Aldrich and used as received. 0.5 mm Silica slides from SPI, Inc. were first cleaned using a 50/50 (v/v) mixture of sulfuric and nitric acid. The silica slides were then rinsed with deionized water (18.2 MΩ/cm) and dried thoroughly to create a fully hydroxylated silica surface that was then affixed to our experimental cell and placed in direct contact with the liquid or saturated vapor phase of interest.

The VSFS apparatus has been described elsewhere.[3] In brief, a Libra-HE Ti:sapphire laser (Coherent, 3.3W 85 fs pulse width, 1kHz repetition rate) coupled to a visible optical parametric amplifier (Coherent OPerA Solo) to generate the visible and IR beams. The IR wavelength was tuned from 3.2 to 3.7 μm in 0.05 μm increments and the IR field was focused

onto the sample at an angle of 73° with respect to normal. The visible beam was spectrally stretched and sliced using an 1800 g/mm grating and variable width slits resulting in a spectrally narrowed visible beam (20 cm^{-1}). After passing through two different delay stages, this beam was focused onto the surface at an angle of 67° with respect to normal. Visible power immediately before the sample was ~8 μJ while the IR power was ~5 μJ. IR power was adjusted with neutral density filters to be as high as possible without boiling the sample. The generated sum frequency signal was directed into a monochromator (SpectraPro-300i, Acton Research Corporation) and dispersed onto a CCD (PIXIS100B, Princeton Instruments). VSF spectra were combined and corrected for ambient background contributions using in-house Igor Pro (v.6) routines.

III. SIMULATION DETAILS

Molecular dynamics simulations of the neat silica-methanol and silica-ethanol solid-liquid interfaces were performed using in-house MD code. Our silica surface is derivative of the fully-hydroxylated β–Cristobalite surface used by Lee and Rossky[34] and has recently been described elsewhere.[35] Briefly, we modified the Lee and Rossky surface to include fully flexible silicon-oxygen-hydrogen surface sites that incorporate the CHARMM water contact angle Lennard-Jones and bond parameters.[36, 37] The methanol and ethanol force field parameters are those used in our earlier work,[38] using a united atom 3 or 4 site description of the alcohol. Intermolecular potentials are calculated as the sum of Lennard-Jones and Coulomb terms:

$$u_{ij}(r) = 4\varepsilon_{ij}\left[\left(\frac{\sigma_{ij}}{r}\right)^{12} - \left(\frac{\sigma_{ij}}{r}\right)^{6}\right] + \frac{q_i q_j}{4\pi r \varepsilon_0} \tag{1}$$

where i and j are atoms of different molecules separated by a distance r. Mixed Lennard-Jones interactions were calculated using standard Lorentz-Berthelot combining rules: $\sigma_{ij} = (\sigma_i + \sigma_j)/2$

and $\varepsilon_{ij} = (\varepsilon_i \varepsilon_j)^{1/2}$. To prepare the adjacent alcohol phases, alcohol molecules were placed in a box with periodic boundary conditions in all directions. The x and y dimensions of this simulation box are set equal to the length and width of the silica surface. The alcohol box height z was allowed to vary so that the correct bulk density of each alcohol is reproduced. The equilibrated box of solvent molecules is then placed adjacent to the silica surface described above. Each silica-alcohol simulation box had dimensions of L_x = 45.0 Å, L_y = 43.3 Å, and L_z = 100 Å with the silica surface placed in the x-y plane at z = 0.0 Å. Silica-alcohol MD simulation boxes contained 90 silanol sites per silica surface (4.62 / nm^2) and 1023 molecules of methanol or 709 molecules of ethanol. Each simulation was equilibrated for a minimum of 1.5 ns prior to initiating production runs. All simulations utilized a time step of 0.5 fs and were performed at 298 K.

Production runs (unless noted otherwise) utilized 10 independently generated configurations, each was used to run a 750 ps MD trajectory at constant T = 298K. Data reported below represents the average over these 7.5 ns of simulation time.

Silica-alcohol hydrogen bond detection utilized a previously described geometrical definition[5] where a silica-alcohol hydrogen bond exists when the donor-acceptor oxygen-oxygen distance, r_{OO}, is less than 3.4 Å and the H-O-acceptor angle is less than 30º.

IV. RESULTS AND DISCUSSION

1. SIMULATION OVERVIEW

Center-of-mass density profiles of liquid methanol and ethanol at a solid silica interface share most features. (Figure 1) The first major peak represents alcohol molecules hydrogen

bonded to the silica surface, in most cases each alcohol molecule at the interface participates in hydrogen bonds with two neighboring silica sites, acting as a hydrogen bond donor in one and as acceptor in the other. The cumulative number of solvent molecules depicted on the right vertical axis shows that the first peak of the density profile of both liquids corresponds to a complete one monolayer coverage of the silica surface. As will be shown below, the alkyl tails of the hydrogen-bonded alcohols align to create a hydrophobic region that repels the polar liquid, resulting in the observed low-density regions that follow the first density peak. This hydrophobic region induces ordering in the alcohols that oscillates for several periods until bulk density is reached at $z \approx 25$Å.
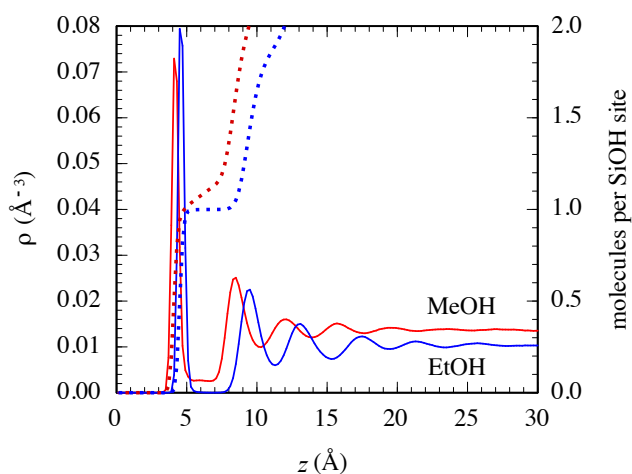
Figure 1. Density profiles of neat methanol (red) and ethanol (blue) at a silica interface. The dotted lines represent the respective cumulative number of solvent molecules per silica surface site (right axis).

The density oscillations are out of phase due to the alcohol molecules' different sizes. The most physically interesting difference is in the region between the first and second major density peaks. In methanol this region is sparsely populated by a small but certainly nonzero

number of molecules, while ethanol exhibits a region of near zero density. This difference is due to the larger alkane-like region formed by ethanol's longer alkyl group. In the silica-methanol system, the surface-induced alkane-like layer is thin enough to not totally repel all non-hydrogen bonded polar molecules in its vicinity. Simulation snapshots in Figure 2 show the difference in the low population regions of the two systems. In this work we shall refer to this low population region between the first two major density peaks as the "second sublayer"[5] and note that this second sublayer is distinct from the *second solvent layer*, which we define as the second major density peak in the respective systems, centered at $z \approx 8$ Å and $z \approx 10$ Å for the methanol and ethanol systems, respectively.
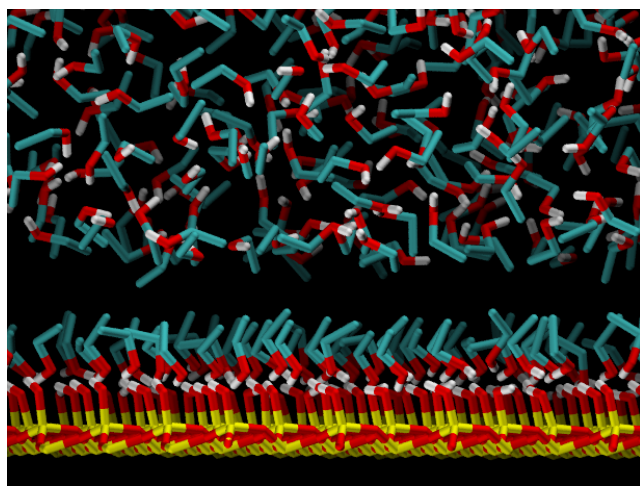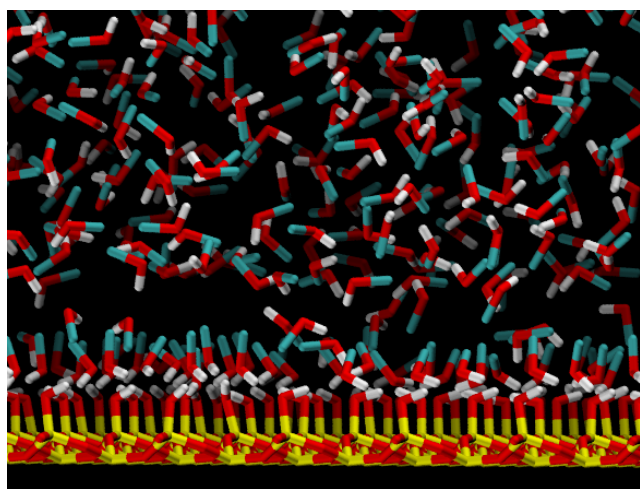
Figure 2. Snapshots of the surface region of methanol (top) and ethanol (bottom) in contact with a silica surface.

Interfacial organization at the surface appears qualitatively similar in both systems but the dynamics of these interfaces, particularly residence time of alcohol molecules near the silica interface, are different. Survival probability quantifies solvent molecule mobility in the direction normal to the silica surface. We define the survival probability as the probability that a molecule of methanol or ethanol within specified lamella parallel to the interface at a given time remains within the same specified region after an elapsed time t. This quantity is calculated using the time correlation function (TCF) formalism:

$$C(t) = \frac{\langle h(t)h(0) \rangle}{\langle h(0)h(0) \rangle} \tag{2}$$

where h represents a random variable of interest. In the case of survival probability, $C_S(t)$, we define h to be 1 if a given molecule is within specified z coordinates and 0 if the molecule is outside of the range. The ensemble average is calculated for all alcohol molecules and for all time origins. These survival probability TCFs, shown in Figure 3, illustrate the relative stability of the silica-ethanol surface. Regions where silica-alcohol hydrogen bonds exist, defined as $0.0 < z < 4.5$ Å and $0.0 < z < 7.0$ Å for methanol and ethanol, respectively, show a large difference in solvent mobility. Methanol's second sublayer is defined as $4.5 < z < 6.0$ Å to include the non-hydrogen bonded molecules adjacent to the methanol molecules hydrogen bonded to the silica surface. As is mentioned above, this second sublayer is distinct from the second solvent layer,

which we define as the second density peak in Figure 1, $7.0 < z < 10.0$ Å. Methanol molecules move in and out of this second sublayer, which enables more surface activity and rearrangement at the interface. The region of near zero density between the first and second ethanol layers does not allow this exchange.
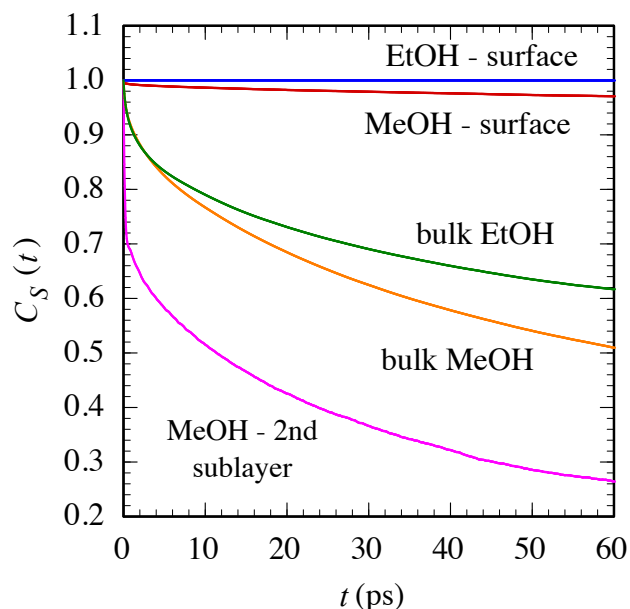
Figure 3. Solvent survival probabilities for the methanol-silica and ethanol-silica systems. Curves represent alcohol-silica interface (surface), alcohol bulk, and second sublayer of methanol behaviors.

The long residence time of the alcohols at the silica surface is due to the formation of silica-alcohol hydrogen bonds. Each alcohol molecule is able to form two separate hydrogen bonds with adjacent hydroxylated silica surface sites where the alcohol acts as hydrogen bond donor in one and acceptor in the other. The hydrogen bond lifetime correlation function, $C_H(t)$, is calculated using Eq. 2. For hydrogen bond lifetimes we define the property h to be 1 if a hydrogen bond exists between a given alcohol-silica pair and 0 if no bond exists. The ensemble

average is calculated over all possible alcohol-silica pairs and all time origins. Hydrogen bonding

correlation functions for the four silica-alcohol interfacial hydrogen bonds are shown in Figure 4.
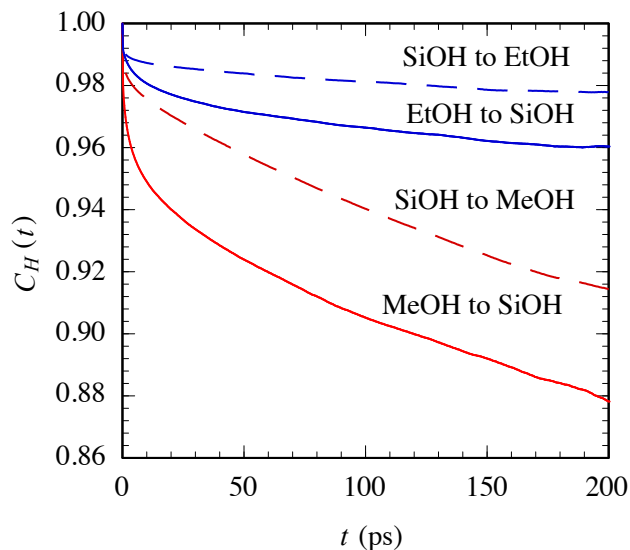
Figure 4. Alcohol-silica hydrogen bond lifetime correlation functions for silica-alcohol

hydrogen bonds. The red curves represent methanol-silica and the blue represent ethanol-silica.

The respective alcohol acts as hydrogen bond donor in the solid curves and as acceptor in the

dashed curves.

Due to the relatively slow dynamics of this interfacial hydrogen bonding we ran longer

simulations to capture these lifetimes, hence the $0 - 200$ ps x-axis in Figure 4. These functions

exhibit rapid decay on the femtosecond time scale representing reoreintational motion of the OH

bond, followed by a slow decay due to translational motion of the alcohols. The slow segments

highlight different behavior based upon the identity of the alcohol and whether the alcohol or

silica acts as hydrogen bond donor. In both cases, ethanol-silica hydrogen bonds are longer lived

than methanol-silica, suggesting more activity and mobility at the methanol-silica interface,

consistent with the survival probability data presented in Figure 3. Specifically, the lack of

ethanol molecules just outside the adsorbed layer lower the probability for hydrogen bond breakup since no "replacement" alcohol molecule is available. Further examination of the lifetime decays reveals that, in both systems, hydrogen bonds are longer lived when the alcohol acts as acceptor (note the smaller slope of the long-time tail of the dashed curve compared with the solid curve for each alcohol). This result can be explained by noting that the silica-hydrogen to alcohol oxygen bond consists of more flexible members than the alcohol hydrogen to silica oxygen bond. Thus, the silica oxygen is considerably less able to accommodate alcohol motion than the silica hydrogen while allowing the hydrogen bond to stay intact.
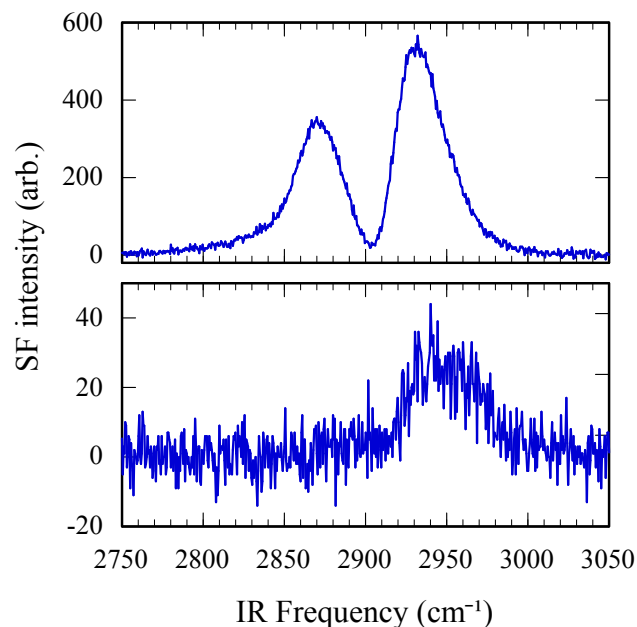
2. VSF SPECTRA

ssp-polarized vibrational sum frequency responses at silica-methanol interfaces are shown in Figure 5. The ssp polarization combination samples those vibrations that have their IR transition dipoles aligned along the surface normal. At the solid-vapor interface (top) two peaks are visible: the methyl symmetric stretch (r^+) centered at 2834 cm^{-1} and a methyl Fermi resonance (r^+-FR) at 2951 cm^{-1}. These data are consistent with what one expects from a methanol monolayer strongly hydrogen bonded to the silica surface with the methanol methyl groups directed towards the vapor phase. The spectrum obtained at the solid-liquid interface (bottom) exhibits no discernible peaks in the same region.
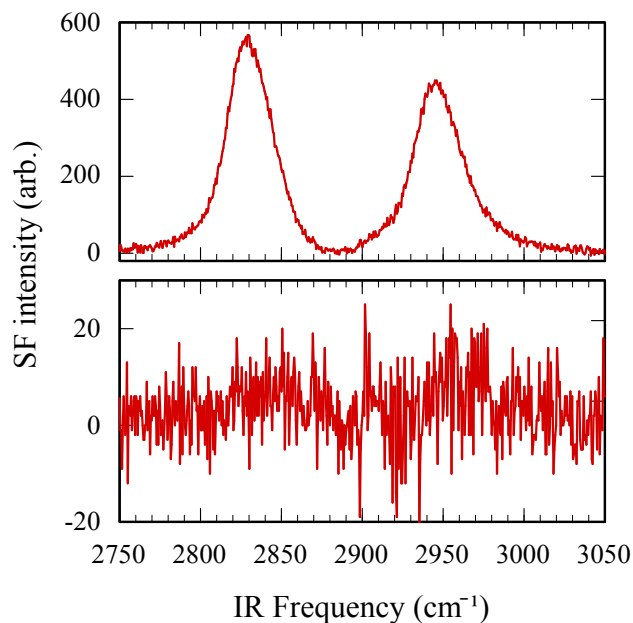
Figure 5. VSF spectra of the silica-methanol solid-vapor (top) and solid-liquid (bottom) interfaces.

VSF spectra from silica-ethanol interfaces (Figure 6) show different behavior. At the silica-ethanol solid-vapor interface (top) the ethanol CH_3 symmetric stretch (r^+) and its associated Fermi Resonance peak (r^+-FR) are observed, centered at 2880 cm^{-1} and 2936 cm^{-1} respectively. In the spectrum from the solid/liquid interface, the low frequency r^+ band disappears and intensity is observed in a broad feature centered at ~2950 cm^{-1} (bottom). Given the absence of r^+ in the spectrum (and a corresponding source of intensity for Fermi resonance coupling), we tentatively assign this broad feature to one of the asymmetric stretches of ethanol's –CH_3 group that no longer has C_{3v} symmetry.[39]

Figure 6. VSF spectra of the silica-ethanol solid-vapor (top) and solid-liquid (bottom) interfaces.

These data present an interesting comparison of how molecular structure affects organization at solid/liquid interfaces. Methanol and ethanol have similar bulk densities, while the static dielectric constants of these solvents differ by less then 25%. Furthermore, methanol and ethanol associate with the silica surface in similar ways. In terms of elements that will influence interfacial solvent organization, the only obvious difference between these two systems is ethanol's additional methyl group. The effect of this difference is apparent both in the solvent density distributions (Figure 1) and in the lifetimes of each solvent's hydrogen bonds (Figure 4) although the solvent survival probabilities (Figure 3) and surface coverages (Figure 1) appear similar.

Experimentally, absolute signal intensities drop (in Figure 6) by approximately an order of magnitude when moving from the solid/vapor interface to the solid/liquid interface. This general attenuation due to the presence of an adjacent liquid phase can be seen in the case of the

ethanol r⁻ mode in Figure 6. Despite this difference in intensities, the absence of any vibrational response from the silica/methanol liquid interface (Figure 5) is striking. Lack of a VSF signal from an interface can arise from several sources: the absence of surface species, isotropic organization at the interface, or strong surface anisotropy having inversion symmetry. At the silica/methanol liquid interface, surface species are present and, given the strength of the methanol-silica hydrogen bonding, a random organization of surface methanol molecules seems unlikely. In the next section, we examine MD simulation results of these systems in an attempt to isolate differences between the silica-methanol and silica-ethanol systems that may illuminate the reason for the suppressed VSFS response in the silica-methanol system.

3. MD INVESTIGTION OF VSFS RESPONSE

To examine VSFS experiments using molecular insight gained from these MD simulations, we consider that an *ssp*-polarized VSF signal arises when the active mode such as the methyl symmetric stretch has a net orientation of its IR transition moment normal to the silica surface. A cumulative orientational profile for the methyl symmetric stretch vector of each solvent is used to visualize the contribution to a VSF signal based solely upon the number of molecules present and their orientation with respect to the silica interface. The cumulative orientational profile $S(z)$ is:

$$S(z) = \sum_{i=0}^{z} N_i \langle \cos\theta \rangle_i \qquad (3)$$

where i represents the index of a discrete bin along the simulation z axis, N is the number of alcohol molecules, and θ is the angle between a vector parallel to molecule's VSF-active mode (in our simulation these vectors are O-CH$_3$ for methanol and CH$_2$-CH$_3$ for ethanol) and a vector

normal to and pointing away from the silica surface. Methanol and ethanol orientational profiles are similarly shaped (Figure 7), both dominated by the orientation induced by alcohol molecules hydrogen bonded to the silica surface.
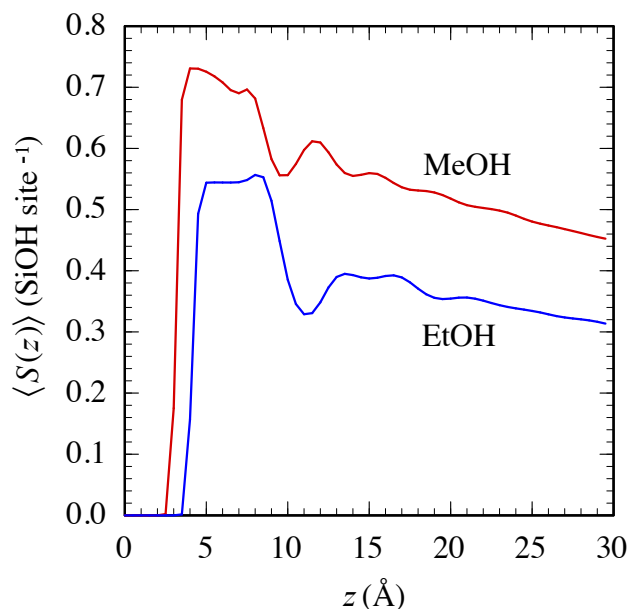
Figure 7. Cumulative orientational profiles of molecular vectors parallel to the VSF-active mode. See Eq 3.

Closer inspection of the two orientational profiles, however, show subtle differences. Methanol's orientational distribution at the interface is more sharply peaked at normal angle than ethanol's, resulting in a profile with larger magnitude despite a similar molecular density at the silica surface. Immediately next to the surface region, ($z = 4$ - 8Å), the curves behave differently. Methanol molecules present in this region (the second sublayer) have negative net orientation, causing a decrease in the curve. For ethanol, this region corresponds to the vacancy between the first and second density peaks that results in a short plateau in the curve. Both curves decrease dramatically at the second density peak and gradually decay as the bulk region is approached,

suggesting a weakly induced orientation of the molecules in a direction opposed to the orientation of the surface molecules.

We next consider the molecular reorientation dynamics using orientational time correlation functions, $C_O(t)$,[40] defined by:

$$C_O(t) = \frac{\langle \hat{u}(t) \cdot \hat{u}(0) \rangle}{\langle \hat{u}(0) \cdot \hat{u}\langle 0 \rangle \rangle} \qquad (4)$$

where $\hat{u}$ is a unit vector parallel to the molecular vector of interest. The ensemble average is calculated over all alcohol molecules and all time origins. Orientational correlation functions of vectors parallel to the VSF active mode are shown in Figure 8.
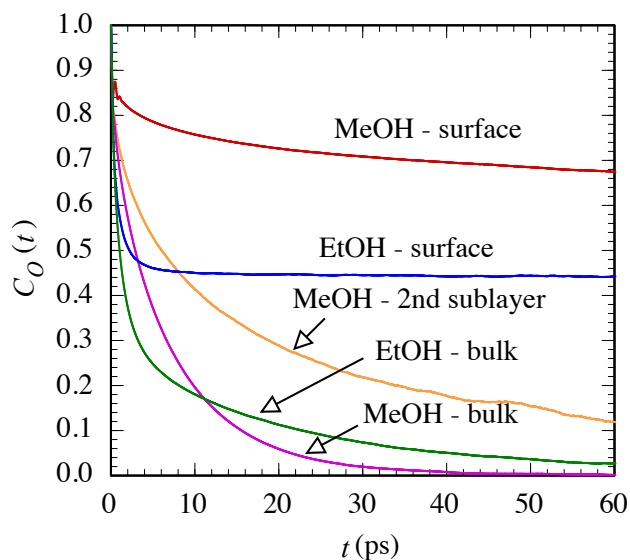

Figure 8. Orientational time correlation functions of the molecular vector parallel to the alcohol's O-CH$_3$ axis.

Alcohol molecules hydrogen bonded to the silica surface exhibit the most limited orientational dynamics. The methanol O-CH$_3$ vector's orientational mobility is limited since

most interfacial methanol act as both hydrogen bond donor and acceptor with silica, essentially fixing the O-CH$_3$ vector. The relevant ethanol vector of interest is affixed to a geometrically similar structure but also able to rotate about the O-CH$_2$-CH$_3$ angle. This condition agrees with the shape of the surface ethanol CH$_2$-CH$_3$ orientational time correlation function and suggests rapid reorientation within a fixed cone. As expected, methanol's second sublayer exhibits a faster reorientation than the hydrogen-bonded methanol at the silica surface but slower than that observed in bulk methanol. We now note that the partial cancelation of the interface-induced order (as shown in Fig. 7) occurs by molecules in the second sublayer that exhibit rapid reorientation dynamics relative to alcohol molecules hydrogen bonded to the silica surface.

The molecular dynamics results with the methanol next to the perfect silica surface suggest that although the methanol molecules directly next to the strongly oriented monolayer are oppositely oriented, the contribution is not dramatic enough to explain the lack of the VSF signal. One possible explanation for this discrepancy is surface structural imperfections that might diminish the signal from the adsorbed monolayer immediately in contact with the silica. To simulate an imperfect silica surface we set the partial charges of every sixth silica site to zero and compared results with the findings previously described. We refer to these surfaces as "deactivated" and "active," respectively. Density profiles of the active and deactivated systems (Figure 9) differ in two main ways. As expected, the number of alcohol molecules hydrogen bonded to the silica surface decreases, as can be seen in the first density peaks and the cumulative numbers in dotted curves. The second difference is a noticeable density increase in the region between the first and second density peaks. The cumulative number of alcohol molecules reveals that the reduced number of surface-bound alcohol molecules is approximately equal to the increased number of molecules present in the "second sublayer."
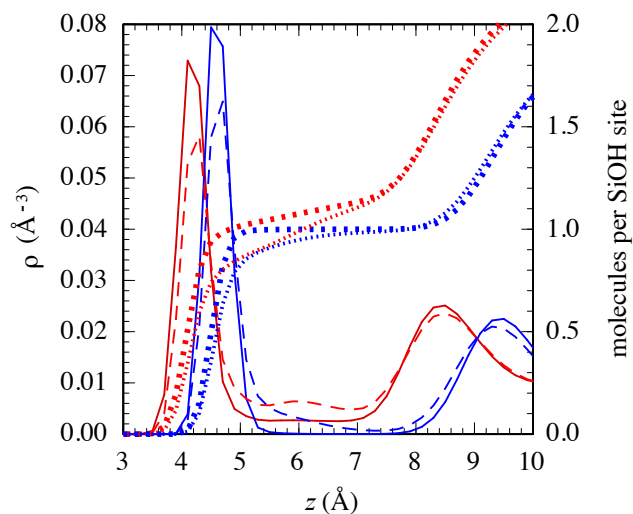
Figure 9. Density profiles of methanol (red) and ethanol (blue) at a silica surface. The solid lines are density profiles at an "active" surface. The dashed curves represent density profiles at a "deactivated" surface. Dotted curves (right axis) represent the integrated densities at "active" (large dots) and "deactivated" (small dots) silica surfaces. (See text for explanation.)

Deactivated silica surfaces change the cumulative orientational profiles of methanol and ethanol systems (see Figure 10). In both systems the initial surface peak is lower due to fewer alcohols hydrogen bonded to the silica surface. More interestingly, we observe that the increased population in the second sublayer acts to further reduce the net orientation. The well-ordered alcohol molecules hydrogen-bonded to the silica surface induce an average orientation in this second sublayer that is opposite to the surface orientation. The impact of this second sublayer is more pronounced in methanol. Finally, as we go beyond the second sublayer region, in the methanol system, the difference between the active and deactivated systems extends toward the bulk, suggesting that disorder in the silica surface results in a greater reduction in the *ssp*-polarized VSF signal from the methyl symmetric stretch than in the ethanol system, whose

"active" and "deactivated" cumulative orientational profiles converge quickly relative to the methanol system.
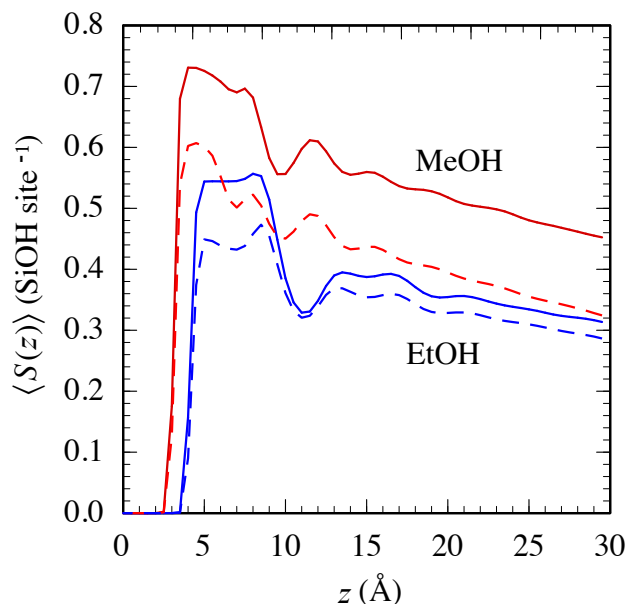

Figure 10. Cumulative orientational profile of methanol (red) and ethanol (blue) at a silica surface, see Eq 3. The solid curves are the corresponding profiles at an "active" surface; the dashed curves correspond to a "deactivated" surface. (See text for explanation.)

Figure 11 supports the above interpretation by showing the orientational distributions of ethanol and methanol molecules at the silica surface as a function of z. Each colored "ribbon" in Figure 11 represents the normalized orientational distribution of the molecules inside a 0.5 Å thick interval along the z-axis and is essentially an expansion of the $\langle \cos\theta \rangle$ term in Eq. 3. The top left plot in Figure 11 shows the orientational distributions of ethanol at the "activated" surface. The region of near zero density in the "activated" ethanol system is noted by making the representative ribbons semi-transparent. When the "deactivated" surface is introduced

(Figure 11, top right) this region sees a rise in population along with fewer interfacial hydrogen-bonded molecules: the ethanol second sublayer is now populated. This ethanol second sublayer displays a stronger induced inversion than in the methanol system (Figure 11, bottom panels). However, unlike the silica-methanol system the orientation of ethanol molecules in the second solvent layer ($7.5 < z < 9.0$ Å, Figure 11, top right) is affected by this population increase. The second solvent layer reorients itself in response to the orientation of the newly populated second sublayer and the net effect is a cumulative orientational profile relatively similar to that of the "activated" system. This induced orientation of the ethanol second solvent layer explains the convergence of the cumulative orientational profiles of ethanol in Figure 10.

The impact of surface defects on the second sublayer offers a possible explanation for the absence of the VSF response from the silica-liquid methanol interface. Surface imperfections increase the population of methanol molecules in the second sublayer. These molecules are orientationaly opposed to the adsorbed molecules, resulting in a diminished signal. Surface defects also increase the population of ethanol molecules in the second sublayer except that in this case – but not for methanol – the ethanol molecules in the second solvent layer adopt an orientation that partially cancels contributions from molecules in the second sublayer. This results in no significant effect on the total signal generated by the silica-ethanol system. Figure 11 describes these induced orientations that result in the different responses seen in Figure 10. In summary, deactivating the silica surface only affects the ethanol response in Figure 10 while $z <$ 10 Å. Deactivating the silica surface in the methanol system introduces a greater *signal reduction* that persists well into the bulk region.
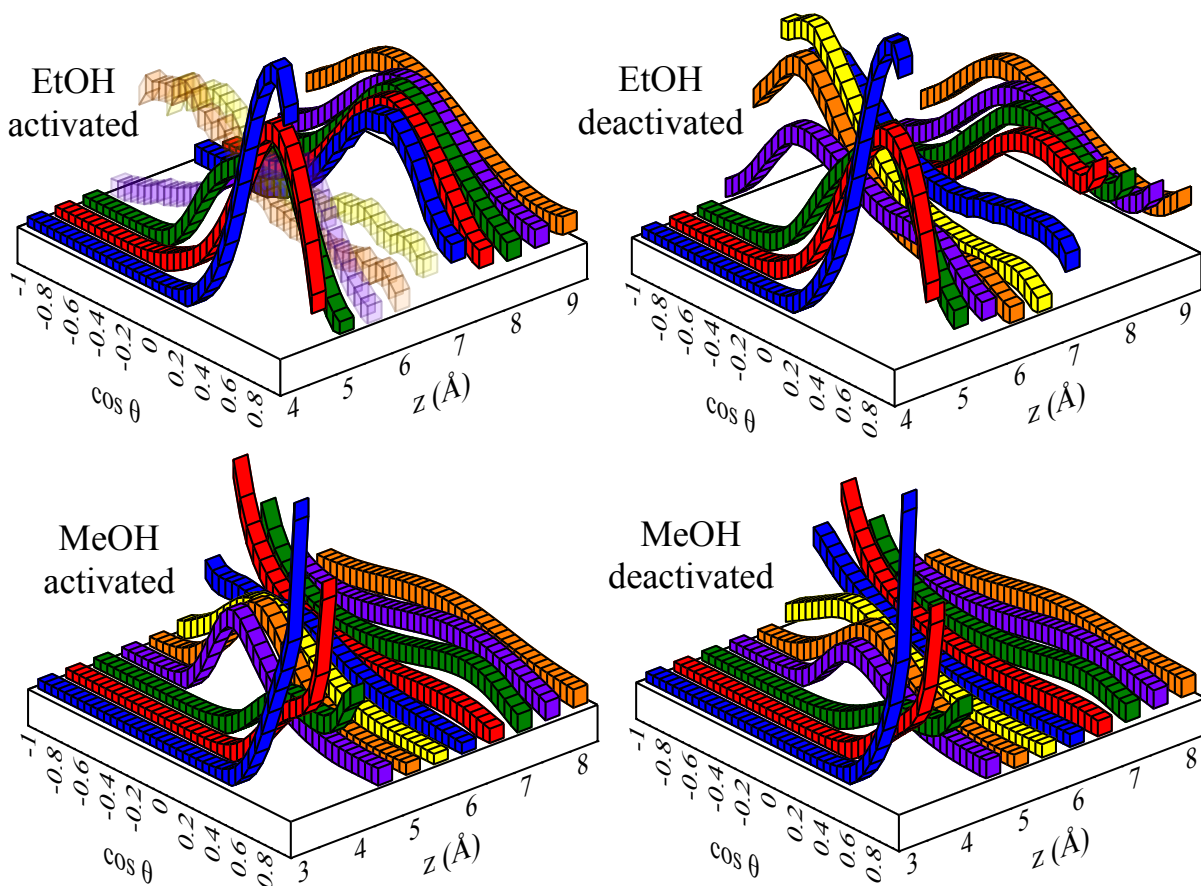
Figure 11. Normalized orientational distributions of ethanol (top) and methanol (bottom) at the "activated" (left) and "deactivated" (right) silica surface.

donor-acceptor	active	deactivated
SiOH-MeOH	3.3	0.71
MeOH-SiOH	3.3	0.57
SiOH-EtOH	23	3.8
EtOH-SiOH	12	2.9

Table 1. Alcohol-silica hydrogen bond lifetimes (ns) for "active" and "deactivated" silica surfaces. (See text for explanation.)

Deactivating surface silica sites also decreases the lifetime of alcohol-silica hydrogen bonds. Silica-alcohol lifetimes obtained by exponential fits of the slow decay parts of the hydrogen bond lifetimes are given in Table 1. These lifetimes were obtained from fit to hydrogen bond lifetime correlation functions calculated from trajectories of longer duration, as mentioned in the discussion of Figure 3 above. We believe that this reduction in lifetime is due to two factors. The deactivated silica sites reduce the probability of alcohol molecules hydrogen bonding to two adjacent silica sites, making the same alcohol-silica interactions half as strong. This increases the likelihood of the molecule leaving the surface. The increased population of the second sublayer in turn increases the likelihood that the surface alcohol molecule will be replaced by a mobile alcohol molecule from this second sublayer.

Tuning the surface hydroxyl composition of silica is difficult to accomplish in a controlled and quantitative manner. However, surface hydroxyl group density can be changed by using a different substrate. α-Alumina is another substrate commonly used in chromatographic applications and as a substrate for packed reactor beds.[41-43] The surface hydroxyl concentration for this metal oxide is estimated to be ~2-3 times higher than for silica.[44-46] Furthermore, α-alumina is considered to have a basic surface compared to silica's acidic surface, meaning that the α-alumina's surface hydroxyl groups will accept even stronger hydrogen bonds from adjacent methanol relative to silica. Given the MD simulation predictions that higher –OH

surface coverage should lead to a stronger SFG response from the liquid-solid interface, we measured the VSF response from a liquid alumina-methanol interface.
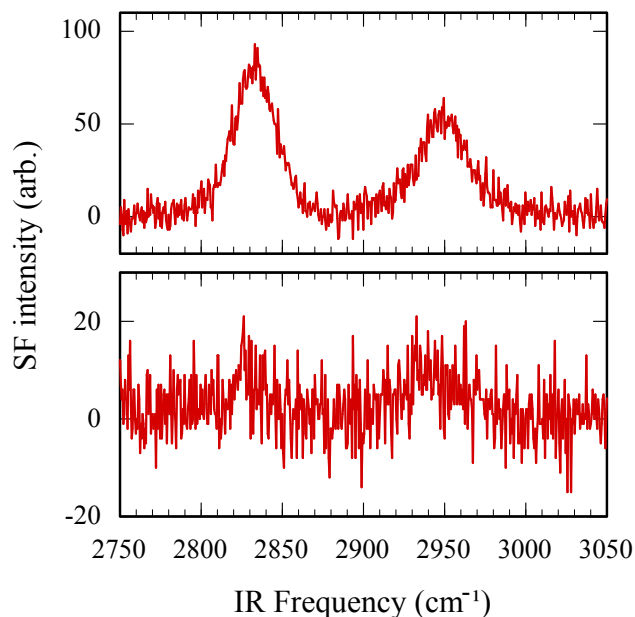
Figure 12. VSF spectra of the alumina-methanol solid-vapor (top) and solid-liquid (bottom) interfaces. Spectra were acquired under *ssp* polarization conditions.

Figure 12 shows that unlike the methanol-silica system (Figure 5), the methanol-alumina liquid-solid interface shows a weak but clearly distinguishable methanol VSF response. Based on insight gained from our experimental and computational studies, we believe this signal is due to the increased surface –OH group density. This increased density of hydroxyl groups manifests itself by diminishing the population and order of the methanol second sublayer. Both of these effects are predicted to lead to an increased SFG signal. This experimental result also raises a host of interesting questions about solvent structure at hydroxyl-terminated surfaces

characterized by different acid-base behaviors. Such questions will be the focus of future studies.

V. CONCLUSIONS

Liquid methanol and ethanol interact with a silica surface by similar means and the silica surface induces a similar molecular order in both liquids. However, VSFS experiments suggest that some non-trivial orientational differences between the two liquid-solid interfaces must exist. We use molecular dynamics simulations of the liquid methanol-silica and liquid ethanol-silica interfaces to compare molecular orientational behavior that may account for the differences in recorded VSF spectra. The single methyl group difference between the alcohols' alkyl groups results in different surface structures. Beyond the hydrogen bonded interface, the aligned methyl tails do not create a large enough hydrophobic region to prevent the formation of a low-density second sublayer that aligns itself to partially cancel the VSF signal. This methanol interlayer has been previously reported[5] and considered as a possible cause of VSF signal attenuation at the methanol-silica surface. This second sublayer is not observed in MD simulations of the ethanol-silica system.

In further studies we introduced defects into the simulated silica surface. This resulted in an ethanol-silica surface with a populated second sublayer region. In these simulations we found that this sublayer induced orientation ethanol's second solvent layer, effectively replacing the average orientational anisotropy negated by molecules present in the second sublayer. *The second solvent layer of methanol does not respond in this manner*. We believe that the lack of induced order in methanol's second solvent layer is largely responsible for the methanol's absent

VSF signal as compared to ethanol's weaker but still present VSF spectrum. The addition of surface defects both increased the population in the second sublayer region and increased the dynamics of the alcohol molecules at the interface.

REFERENCES

1.	Bain, C. D. Sum-Frequency Vibrational Spectroscopy of the Solid-Liquid Interface. *J. Chem. Soc.-Faraday Trans.* **1995,** *91* (9), 1281-1296.

2.	Benjamin, I. Chemical Reactions and Solvation at Liquid Interfaces: A Microscopic Perspective. *Chem. Rev.* **1996,** *96* (4), 1449-1475.

3.	Gobrogge, E. A.; Woods, B. L.; Walker, R. A. Liquid Organization and Solvation Properties at Polar Solid/Liquid Interfaces. *Faraday Discuss.* **2013,** *167*, 309-327.

4.	Liu, X. Y.; Bennema, P. The Relation between Macroscopic Quantities and the Solid-Fluid Interfacial Structure. *J. Chem. Phys.* **1993,** *98* (7), 5863-5872.

5.	Roy, D.; Liu, S. L.; Woods, B. L.; Siler, A. R.; Fourkas, J. T.; Weeks, J. D.; Walker, R. A. Nonpolar Adsorption at the Silica/Methanol Interface: Surface Mediated Polarity and Solvent Density across a Strongly Associating Solid/Liquid Boundary. *J. Phys. Chem. C* **2013,** *117* (51), 27052-27061.

6.	Vieceli, J.; Benjamin, I. Adsorption at the Interface between Water and Self-Assembled Monolayers: Structure and Electronic Spectra. *J. Phys. Chem. B* **2002,** *106* (32), 7898-7907.

7.   Escudero, C.; Salmeron, M. From Solid-Vacuum to Solid-Gas and Solid-Liquid

Interfaces: In Situ Studies of Structure and Dynamics under Relevant Conditions. *Surf. Sci.* **2013,**

607, 2-9.

8.   Bond, G. C.; Thompson, D. T. Catalysis by Gold. *Catal. Rev.-Sci. Eng.* **1999,** *41* (3-4),

319-388.

9.   Diebold, U. The Surface Science of Titanium Dioxide. *Surf. Sci. Rep.* **2003,** *48* (5-8), 53-

229.

10.   Prime, K. L.; Whitesides, G. M. Self-Assembled Organic Monolayers - Model Systems

for Studying Adsorption of Proteins at Surfaces. *Science* **1991,** *252* (5009), 1164-1167.

11.   Smith, R. K.; Lewis, P. A.; Weiss, P. S. Patterning Self-Assembled Monolayers. *Prog.*

Surf. Sci. **2004,** *75* (1-2), 1-68.

12.   Parida, S. K.; Dash, S.; Patel, S.; Mishra, B. K. Adsorption of Organic Molecules on

Silica Surface. *Adv. Colloid Interface Sci.* **2006,** *121* (1-3), 77-110.

13.   Whitesides, G. M.; Laibinis, P. E. Wet Chemical Approaches to the Characterization of

Organic-Surfaces - Self-Assembled Monolayers, Wetting, and the Physical Organic-Chemistry

of the Solid Liquid Interface. *Langmuir* **1990,** *6* (1), 87-96.

14.   Miranda, P. B.; Shen, Y. R. Liquid Interfaces: A Study by Sum-Frequency Vibrational

Spectroscopy. *J. Phys. Chem. B* **1999,** *103* (17), 3292-3307.

15.   Du, Q.; Freysz, E.; Shen, Y. R. Vibrational-Spectra of Water-Molecules at Quartz Water

Interfaces. *Phys. Rev. Lett.* **1994,** *72* (2), 238-241.

16.   Ding, F.; Hu, Z. H.; Zhong, Q.; Manfred, K.; Gattass, R. R.; Brindza, M. R.; Fourkas, J.

T.; Walker, R. A.; Weeks, J. D. Interfacial Organization of Acetonitrile: Simulation and

Experiment. *J. Phys. Chem. C* **2010,** *114* (41), 17651-17659.

17.   Hopkins, A. J.; McFearin, C. L.; Richmond, G. L. Investigations of the Solid-Aqueous Interface with Vibrational Sum-Frequency Spectroscopy. *Curr. Opin. Solid State Mat. Sci.* **2005,** *9* (1-2), 19-27.

18.   Ong, S. W.; Zhao, X. L.; Eisenthal, K. B. Polarization of Water-Molecules at a Charged Interface - 2nd Harmonic Studies of the Silica Water Interface. *Chem. Phys. Lett.* **1992,** *191* (3-4), 327-335.

19.   Ostroverkhov, V.; Waychunas, G. A.; Shen, Y. R. New Information on Water Interfacial Structure Revealed by Phase-Sensitive Surface Spectroscopy. *Phys. Rev. Lett.* **2005,** *94* (4), 4.

20.   Liu, W. T.; Zhang, L. N.; Shen, Y. R. Interfacial Layer Structure at Alcohol/Silica Interfaces Probed by Sum-Frequency Vibrational Spectroscopy. *Chem. Phys. Lett.* **2005,** *412* (1-3), 206-209.

21.   Wittcoff, H. A.; Reuben, B. G. *Industrial Organic Reactions*. J. Wiley: New York, 1996.

22.   Seddon, D. Reformulated Gasoline, Opportunities for New Catalyst Technology. *Catal. Today* **1992,** *15* (1), 1-21.

23.   Natal-Santiago, M. A.; Dumesic, J. A. Microcalorimetric, Ftir, and DFT Studies of the Adsorption of Methanol, Ethanol, and 2,2,2-Trifluoroethanol on Silica. *J. Catal.* **1998,** *175* (2), 252-268.

24.   Pelmenschikov, A. G.; Morosi, G.; Gamba, A.; Zecchina, A.; Bordiga, S.; Paukshtis, E. A. Mechanisms of Methanol Adsorption on Silicalite and Silica - Ir-Spectra and Ab-Initio Calculations. *J. Phys. Chem.* **1993,** *97* (46), 11979-11986.

25.   Kanda, Y.; Nakamura, T.; Higashitani, K. Afm Studies of Interaction Forces between Surfaces in Alcohol-Water Solutions. *Colloid Surf. A-Physicochem. Eng. Asp.* **1998,** *139* (1), 55-62.

26.   Mizukami, M.; Moteki, M.; Kurihara, K. Hydrogen-Bonded Macrocluster Formation of Ethanol on Silica Surfaces in Cyclohexane. *J. Am. Chem. Soc.* **2002,** *124* (43), 12889-12897.

27.   Gobrogge, E. A.; Walker, R. A. Binary Solvent Organization at Silica/Liquid Interfaces: Preferential Ordering in Acetonitrile-Methanol Mixtures. *J. Phys. Chem. Lett.* **2014,** *5* (15), 2688-2693.

28.   Zhang, L. N.; Liu, W. T.; Shen, Y. R.; Cahill, D. G. Competitive Molecular Adsorption at Liquid/Solid Interfaces: A Study by Sum-Frequency Vibrational Spectroscopy. *J. Phys. Chem. C* **2007,** *111* (5), 2069-2076.

29.   Barnette, A. L.; Kim, S. H. Coadsorption of N-Propanol and Water on Sio2: Study of Thickness, Composition, and Structure of Binary Adsorbate Layer Using Attenuated Total Reflection Infrared (Atr-Ir) and Sum Frequency Generation (SFG) Vibration Spectroscopy. *J. Phys. Chem. C* **2012,** *116* (18), 9909-9916.

30.   Siler, A. R.; Walker, R. A. Effects of Solvent Structure on Interfacial Polarity at Strongly Associating Silica/Alcohol Interfaces. *J. Phys. Chem. C* **2011,** *115* (19), 9637-9643.

31.   Zhang, X.; Steel, W. H.; Walker, R. A. Probing Solvent Polarity across Strongly Associating Solid/Liquid Interfaces Using Molecular Rulers. *J. Phys. Chem. B* **2003,** *107* (16), 3829-3836.

32.   Brindza, M. R.; Walker, R. A. Differentiating Solvation Mechanisms at Polar Solid/Liquid Interfaces. *J. Am. Chem. Soc.* **2009,** *131* (17), 6207-6214.

33.   Melnikov, S. M.; Holtzel, A.; Seidel-Morgenstern, A.; Tallarek, U. Evaluation of Aqueous and Nonaqueous Binary Solvent Mixtures as Mobile Phase Alternatives to Water-Acetonitrile Mixtures for Hydrophilic Interaction Liquid Chromatography by Molecular Dynamics Simulations. *J. Phys. Chem. C* **2015,** *119* (1), 512-523.

34.   Lee, S. H.; Rossky, P. J. A Comparison of the Structure and Dynamics of Liquid Water at Hydrophobic and Hydrophilic Surfaces—a Molecular Dynamics Simulation Study. *J. Chem. Phys.* **1994,** *100* (4), 3334-3345.

35.   Karnes, J. J.; Benjamin, I. Mechanism and Dynamics of Molecular Exchange at the Silica/Binary Solvent Mixtures Interface. *J. Phys. Chem. A* **119**, ASAP (2015).

36.   Cruz-Chu, E. R.; Aksimentiev, A.; Schulten, K. Water-Silica Force Field for Simulating Nanodevices. *J. Phys. Chem. B* **2006,** *110* (43), 21497-21508.

37.   Leroch, S.; Wendland, M. Simulation of Forces between Humid Amorphous Silica Surfaces: A Comparison of Empirical Atomistic Force Fields. *J. Phys. Chem. C* **2012,** *116* (50), 26247-26261.

38.   Benjamin, I. Vibrational Spectrum of Water at the Liquid/Vapor Interface. *Phys. Rev. Lett.* **1994,** *73* (15), 2083-2086.

39.   Weldon, M. K.; Uvdal, P.; Friend, C. M.; Serafin, J. G. Decoupling of Vibrational Modes as a Structural Tool: Coverage−Induced Reorientation of Methoxide on Mo(110). *J. Chem. Phys.* **1995,** *103* (12), 5075-5084.

40.   Burshtein, A. I.; Temkin, S. I. *Spectroscopy of Molecular Rotation in Gases and Liquids*. Cambridge University Press: 2005.

41.   Nawrocki, J.; Dunlap, C.; McCormick, A.; Carr, P. W. Part I. Chromatography Using Ultra-Stable Metal Oxide-Based Stationary Phases for HPLC. *J. Chromatogr. A* **2004,** *1028* (1), 1-30.

42.   Grün, M.; Kurganov, A. A.; Schacht, S.; Schüth, F.; Unger, K. K. Comparison of an Ordered Mesoporous Aluminosilicate, Silica, Alumina, Titania and Zirconia in Normal-Phase High-Performance Liquid Chromatography. *J. Chromatogr. A* **1996,** *740* (1), 1-9.

43.   Claessens, H. A.; van Straten, M. A. Review on the Chemical and Thermal Stability of Stationary Phases for Reversed-Phase Liquid Chromatography. *J. Chromatogr. A* **2004,** *1060* (1–2), 23-41.

44.   Digne, M.; Sautet, P.; Raybaud, P.; Euzen, P.; Toulhoat, H. Hydroxyl Groups on γ-Alumina Surfaces: A DFT Study. *J. Catal.* **2002,** *211* (1), 1-5.

45.   Wischert, R.; Florian, P.; Copéret, C.; Massiot, D.; Sautet, P. Visibility of Al Surface Sites of γ-Alumina: A Combined Computational and Experimental Point of View. *J. Phys. Chem. C* **2014,** *118* (28), 15292-15299.

46.   Iwasawa, Y. *Catalysis by Metal Complexes*. D. Reidel Publishing Company: Dordecht, Holland, 1986; Vol. 7.

Table of Contents Graphic.